High strain rate behaviour of renewable biocomposites based on dimer fatty acid polyamides and cellulose fibres

Rodrigue Matadi, Elodie Hablot, Kui Wang, Nadia Bahlouli, Said Ahzi, Luc Avérous

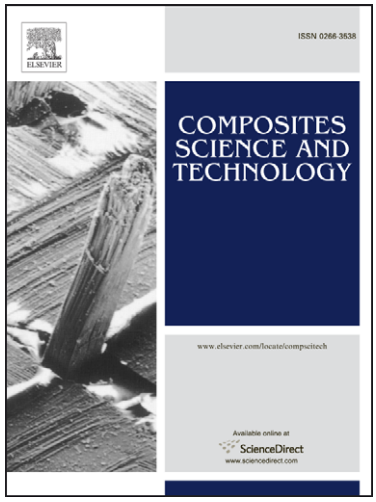

High strain rate behaviour of renewable biocomposites based on dimer fatty acid polyamides and cellulose fibres

Rodrigue Matadi, Elodie Hablot, Kui Wang, Nadia Bahlouli, Said Ahzi, Luc Avérous

PII: S0266-3538(11)00038-8
DOI: 10.1016/j.compscitech.2011.01.010
Reference: CSTE 4905

To appear in: *Composites Science and Technology*

Received Date: 28 October 2010
Revised Date: 13 January 2011
Accepted Date: 16 January 2011

Please cite this article as: Matadi, R., Hablot, E., Wang, K., Bahlouli, N., Ahzi, S., Avérous, L., High strain rate behaviour of renewable biocomposites based on dimer fatty acid polyamides and cellulose fibres, *Composites Science and Technology* (2011), doi: 10.1016/j.compscitech.2011.01.010

High strain rate behaviour of renewable biocomposites based on dimer fatty acid polyamides and cellulose fibres

Rodrigue Matadi[1], Elodie Hablot[2], Kui Wang[1], Nadia Bahlouli[1], Said Ahzi[1], Luc Avérous[2*]

[1] *Institut de Mécanique des Fluides et des Solides, IMFS Université de Strasbourg, Strasbourg, 2 rue Boussingault, 67000 Strasbourg, France*

[2] *Laboratoire d'Ingénierie des Polymères pour les Hautes Technologies, LIPHT-ECPM, EAc 4379(CNRS), Université de Strasbourg, 25 rue Becquerel, 67087 Strasbourg, Cedex 2, France*

Abstract: Replacing petroleum-based raw materials with renewable resources is now a major concern in terms of economical and environmental viewpoints. New innovative and biosourced polyamides based on dimer fatty acid (DAPA), and its composites (DAPAC) with pure cellulose short fibres (CF) were elaborated. The understanding of the mechanical behaviour of these new biomaterials is essential to consider their future applications. The high strain rate behaviour of DAPA and DAPAC were studied using split Hopkinson pressure bars (SHPB). Dynamic test were made for different strain rate and various temperatures. The dynamic properties results show an enhancement of the Young's modulus, the yield stress, and the flow stress with increasing CF content. It was also found that both systems, neat DAPA and DAPAC, are highly thermo-dependent and mechanically sensitive. The increase of strain rate leads to the increase of polymer flow, with a very significant increase of strain hardening, indicating that the addition of CF does not change the ability of DAPA to plastically deform. The addition of CF has no remarkable effect on the strain rate sensitivity. The results also shows that the effective activation energy increase slightly with the CF content. Besides, the effective activation volume decreases slightly with increasing CF concentration, indicating that the chains mobility are relatively reduced in presence of filler. A micromechanically-model known as cooperative model based on the assumption that the yield stress is a thermal activation processes and the yield stress obeys to the strain rate /temperature superposition principle, was used to predict the dynamic compressive yield stress of both DAPA and DAPAC. The prediction of the yield stress is in very good agreement with the experimental data.

Keywords: A. Fibres, A. Short-fibre composites, C. Mechanical properties, C. Modelling, Dynamic Compression

1. INTRODUCTION

The use of agro-based products to replace common petroleum-based plastics becomes of great interest because of the diminishing fossil resources combined with the global and increasing environmental concern [1]. Vegetable oils, which are renewable resources present in abundance throughout the world, are expected to be an ideal alternative chemical feedstock to develop new environmentally friendly materials [2-8]. Dimer fatty acids (DA), which can be issued from dimerization of fatty acids of soybean oil, are well-known and commercially available product [9-11]. Thus, they are good candidates to form new bio-based thermoplastic polyamides [9, 11-14]. Soy-based polyamides (DAPA), due to their special macromolecular architecture based on dimer fatty acids, show relatively good performances [11]. But they are still rather far from conventional thermoplastic polyamides' properties. Then, an effective approach to improve the behaviour of these polyamides, described in previous works [11, 15-16], is the incorporation of short cellulose fibres (CF) in the DAPA matrix to produce biocomposites (DAPAC).

Several researches [17-19] have investigated the elaboration and the mechanical characterization of biobased polymers using different approaches. These studies are focused on epoxy resins from vegetable oil. For instance, Lui et al [20-22] have reported the synthesis of epoxidized soybean oil/epoxy nanocomposites with different amines curing agents. This previous work is only focused on the elaboration and the experimental characterization of their physical and

mechanical properties at low strain rate. Moreover, several studies on high strain rate behaviour of wood have been investigated [23-24].

However, as of today, the high strain-rate mechanical properties of thermoplastic biobased polymers and their corresponding composites have never been investigated yet.

The aim of this work is to study the compressive dynamic behaviour of DAPA and DAPAC with different filler contents. The mechanical behaviour at high strain rate was analysed and the compressive dynamic yield stress was then investigated and modelled with a cooperative model, to predict the corresponding mechanical evolution [25-28]. This work completes our previous studies on the elaboration, the structure, and the physico-chemical properties of DAPA and DAPAC as well as the modelling of the Young modulus and the Yield behaviour have been investigated [15-16].

2. EXPERIMENTAL

2.1. Materials

Dimer acid used in the synthesis is supplied by Prolea (France). Radiacid 0970 is a yellowish, viscous liquid at room temperature with the dimer, trimer and monomer content at 96.6, 2.8 and 0.6 wt%, respectively. Radiacid 0970 dimer fatty acid is partially hydrogenated to improve its stability. It presents an iodine value of 25 mgKOH/100 g, which corresponds to 0.2 double bonds per molecule. 1,6-diaminohexane,and all the chemicals were purchased from Sigma Aldrich and used as received.

Pure cellulose fibres (CF), issued from leaf wood, are used in this study. This product, Arbocel B400, is supplied by JRS (Rosenberg, Germany). According to this supplier, they show an average length and thickness of 900 and 20 μm, respectively. In a previous paper, Amash et al.

[29] have presented some characteristics of these fibres. According to these authors, the density of the fibres is 1.50 and the cellulose content is greater than 99.5 %.

2.2. Polyamides Synthesis

As described in previous publications [11, 15-16], this new biobased polyamide (DAPA) is synthesized by condensation polymerization. Dimer acid is charged in a 1L five-necked round-bottom flask equipped with mechanical stirrer, a thermometer, a nitrogen inlet, a Dean-Stark apparatus and a dropping funnel. Dimer acid is heated at 50 °C under stirring and nitrogen atmosphere. 1,6-diaminohexane equivalent to total acid equivalent is added by using dropping funnel during 10 min. After 1,6-diaminohexane addition, the mixture is heated gradually to 180 °C within 3 hours. The completion of the polymerization is checked by amine and acid titration. The reaction is stopped after the consumption of more than 99 % of the acid groups. The final thermoplastic polyamide is then discharged from the flask. Additional details are given in a previous work [15].

DAPA is yellowish, transparent and flexible at ambient temperature with a molecular weight of 14 000 g/mol, a glass transition temperature of -10 °C and a fusion temperature of 81 °C.

2.3. Composites processing

Prior to blending, fibres and DAPA are dried in an air-circulating oven during 60 min. at 110 and 70 °C, respectively. DAPA and varying amounts of CF are added in the feeding zone of an internal mixer (Counterrotating mixer Rheocord 9000, Haake, USA) at 100 °C, with a rotation speed of 50 rpm and a maximum processing time of 8 min, to avoid DAPA degradation. Three biocomposites (DAPAC) are prepared with 5 and 10 and 15 wt.%, of CF, and named DAPAC5, DAPAC10 and DAPAC15, respectively. After melt processing, the materials are compression-

molded, to obtain films or plates, with a hot press at 130 °C applying 200 MPa pressure for 5 min. The molded specimens are then quenched between two steel plates for 10 min at room temperature.

The fibres dispersion in DAPA matrix was then evaluated [15]. The results showed a good dispersion of CF in the matrix. Filler and matrix affinity was also evaluated. On SEM micrographs obtained from cryogenic fracture of DAPAC15 (see fig 1), we can see that a majority of fibres are cut at the level of the sample surface. However, some holes, corresponding to fibres totally pulled out from the matrix, can also be observed, which shows a limited compatibility between CF and DAPA.

2.4. Dynamic mechanical properties

To investigate materials' mechanical behaviour, two typical devices are used to perform a wide range of strain rates. The mechanical behaviour at low and moderate strain rates in most case are characterized by tensile tests with an Instron or a MTS servohydraulic test system [8, 30]. In the field of high strain rates, most researchers work with a split Hopkinson pressure bar (SHPB) for the compression tests. In this paper, the high strain rate properties were characterized with a homemade SHPB [31], with a diameter of 22 mm. This device includes three parts: an incident bar, a transmission bar and a striker bar with a length of 3 m, 3 m and 1 m, respectively. To heat the samples, a small furnace has been developed with two symmetrical resistance heaters, which can reach 200 °C in a few minutes. Four thermocouples were inserted to measure and control the temperature distribution in the furnace and to ensure that all tests were carried out under the same experimental conditions.

With the purpose of investigating the dynamic thermomechanical behaviour, cylindrical specimens with a diameter of 8 mm and a thickness of 3 mm, cut from compression moulding plates, have been tested. The relative smaller size of specimens could reduce inertial stresses to reach and relative easily the stress equilibrium during a high strain rate test [32]. Dynamic compressive tests were carried out at four strain rates ($\dot{\varepsilon}_1 = 413 \pm 6.2\%$, $\dot{\varepsilon}_2 = 913 \pm 4.2\%$, $\dot{\varepsilon}_3 = 1735 \pm 2.3\%$, $\dot{\varepsilon}_3 = 2730 \pm 2.7\%$), which will be called Strain Rate 1, 2, 3 and 4 , respectively) and at three temperatures before the melting temperature (20 °C, 40 °C and 60 °C).

The materials' dynamic mechanical behaviour tests which were performed on SHPB device could be subject to three major experimental errors that include friction with the two flat-ended bars and a radial inertia [33]. Some preliminary studies have been done by Walley et al. [34], who suggest that when the aspect ratio L/D is greater than 0.12, we can ignore the effect of friction. Then, the cylindrical specimens have been tested without lubrication.

3. RESULTS AND DISCUSSION

3.1. Cellulose content effect

Stress strain curves of DAPA and DAPAC at various cellulose contents for a given temperature and strain rate are shown in Fig. 2, 3 and 4. As a first observation, it can be noticed that the stress-strain curves of DAPA and DAPAC can be divided into different stages, depending on the level of strain rate. At strain rate 1, two stages can be observed with an initial linear elasticity followed by a non-linear transition to global yield stress. Whereas the stress-strain curves are composed by 3 stages, for Strain Rate 2. As for Strain Rate 1, we can show an initial linear elasticity, a non linear transition to yield stress. Besides, in this case a flow at constant stress is

shown. For strain rate ranging from Strain Rate 3 to Strain Rate 4, in addition to what is observed at Strain Rate 2, fourth and fifth parts are noticed corresponding to strain softening and hardening, respectively. This plastic behaviour part is wider at strain rate of 2700 s^{-1} (Strain Rate 4), showing that when the strain rate increases, the strain hardening effect of DAPA and DAPAC also increases. Obviously, all the mechanical properties dramatically go up as the strain rate increases. The most evident is the strain hardening which increases significantly with the strain rate. Chen et al. [35] believe that this stress increase has a closer relationship to the secondary molecular process. In fact an increasing strain rate leads to the restriction of the beta movements of the polymer chains by preventing their relaxation. As the strain rate increases, the effect of strain hardening decreases slightly at high cellulose contents. This effect may be linked to the presence of areas of stresses concentrations caused by the agglomeration of fibers at high concentrations, as can be seen on Fig. 5. Cellulose fibres don't seem to reduce the strain at break, indicating the ability of DAPA and DAPAC to plastically deform. This behaviour is probably due to the relatively low glass transition temperature of the studied systems (From -10 °C to -1 °C for DAPA and DAPAC15, respectively), largely below the test temperature.

It is also revealed from these results, that the Young's modulus, the yield stress and the flow stress increase with the cellulose contents. In Fig 2, e.g., the results obtained at 20 °C and at strain rates of 413 s^{-1} (strain rate 1) show that the Young's modulus varies from 465 MPa for the neat DAPA to 541 MPa, 611 MPa and 695 MPa for DAPAC5, DAPAC10 and DAPAC15, respectively. Besides, the yield stress increases from 31 MPa for DAPA to 36 MPa, 40 MPa and 43 MPa for DAPAC5, DAPAC10 and DAPAC15, respectively. Table 1 summarizes the Young's modulus and yield stress values of DAPA and DAPAC for different cellulose concentrations, strain rates, and temperatures. Then, the mechanical increase (Table 1) is mainly due both to the good fibre dispersion in the matrix and to the relative good fire/matrix interfacial interactions. In

fact the fibre presents a very high Young's modulus compared to that of the matrix. When the filler distribution is high, the fibre/matrix interfaces are increased and in this way the percentage of borne stress is increased.

3.2. Strain rate and temperature effects

Fig. 6 shows both strain rate and temperature effect on the mechanical properties of DAPA and DAPAC. According to the results depicted on Fig 6, both systems are very sensitive to the strain rate and temperature. Obviously, the Young's modulus, yield stress and flow stress of DAPA and DAPAC significantly increase with the strain rate. For example, for neat DAPA tested at 20 °C, the Young's modulus rises from 465 to 603 MPa and the yield stress increases from 31 to 60 MPa, with an increase of the strain rate from 413 to 2730 s^{-1}, respectively. This phenomenon is mainly due to the fact that increasing strain rate induced a decrease of the chains mobility and thus increase the material stiffness [36]. The dependence of compressive Young's modulus on strain rate is shown in Fig 7. Young's modulus of DAPA and DAPAC tended to increase significantly and linearly with the strain rate (Fig 7). At low temperature (20 °C), the addition of fibres seems to have no effect on the strain rate sensitivity of Young's modulus (see Fig 7). This observation is shown with the evolution of Young's modulus as a function of strain rate, which presents at this temperature a series of parallel lines. When the temperature increases, this parallelism is lost. The addition of cellulose fibres has lower effect on the strain rate sensitivity of the yield stress (see Fig 8). For instance, for DAPAC10 tested at 20 °C, the yield stress varies from 40 to 76 MPa with an increase of the strain rate from 413 s^{-1} to 2730 s^{-1}, respectively. That approximately equals to the increasing rate of yield stress of neat DAPA taken at the same strain rates and temperature. This behaviour is in agreement with all the results presented in Fig 8 where the yield stress of DAPA and DAPAC, with different cellulose contents were plotted as a function of strain rate at a given temperature. As illustrated in Fig 8, at a temperature of 20 °C

the evolution of yield stress as a function of strain rate for different materials represents a series of parallels lines, showing that both DAPA and DAPAC have the same strain rate sensitivity. This behaviour was also observed at 40 °C and 60 °C.

3.3. Yield stress modelling

Following the recent works [16, 25-28], the temperature and strain rate dependence of yield behaviour of different polymers can be described and estimated by the cooperative model where the yield stress σ_y is expressed below T_g according eq. 1. T is the absolute temperature, k the Boltzmann constant, V_{eff} an effective activation volume, ΔH_{eff} an effective activation energy, $\dot{\varepsilon}$ the strain rate, $\dot{\varepsilon}_0$ a pre-exponential constant, $\sigma_i(0)$ the internal stress at 0K; m a material parameter equal to $\sigma_i(0)/T^*$, T^* being the compensation temperature and n describes the cooperative character of the yield process [29].

$$\frac{\sigma_y}{T} = \frac{\sigma_i(0) - m \cdot T}{T} + \frac{2k}{V_{eff}} \sinh^{-1}\left(\frac{\dot{\varepsilon}}{\dot{\varepsilon}_0 \exp\left(-\frac{\Delta H_{eff}}{kT} \right)} \right)^{1/n} \qquad (1)$$

Chivrac et al. [25] and Gueguen et al. [26] have shown that the Takayanagi model [37] can be used to estimate the effective activation volume and effective activation energy according to the Eq. 2, where φ and Ω are parameters related to the volume fractions of the DAPA matrix

$$\begin{aligned} \Delta H_{eff} &= \frac{\varphi \cdot \Delta H_C \cdot \Delta H_D}{\Omega \cdot \Delta H_D + (1-\Omega) \cdot \Delta H_C} + (1-\varphi) \cdot \Delta H_D \\ V_{eff} &= \frac{\varphi \cdot V_C \cdot V_D}{\Omega \cdot V_D + (1-\Omega) \cdot V_C} + (1-\varphi) \cdot V_D \end{aligned} \qquad (2)$$

The volume fractions of DAPA(f_D) and cellulose fibres (f_C) are given by the eq. 3.

$$\begin{cases} f_C = \varphi \cdot \Omega \\ f_D = 1 - \varphi \cdot \Omega \end{cases} \qquad (3)$$

The micromechanically-based cooperative approach (Equations 1 and 2) has been applied to model and then predict the compressive yield behaviour of DAPA and DAPAC. The biocomposite is considered as a two phases material (matrix and fibres). The yield processes in each phase are described by the activation parameters of the DAPA matrix (ΔH_D and V_D) and those of the cellulose fillers (ΔH_C and V_C).

For the model parameter determination, we chose first to calculate the model parameters for DAPA, by using both Ree-Eyring and Richeton equations. Then the model parameters for DAPA/Cellulose biocomposites are obtained from the works of Chivrac et al. [25] and Matadi et al. [16] on the yield behaviour of polymers nanocomposites. Because of both cooperative and the Ree-Eyring models consider the same β activation energy; we chose in this study to calculate the activation energy and the activation volume of DAPA by using an asymptotic development of the Ree-Eyring formulation given by the equation (4):

$$\sigma_y = \frac{2\Delta H}{V} + \frac{2kT}{V} \ln\left(\frac{2\dot{\varepsilon}}{\dot{\varepsilon}_0}\right) \qquad (4)$$

Temperature-normalized yield stress (σ_y / T) against logarithmic strain rate sets a series of parallel, linear isotherms with a constant activation energy (ΔH) and an activation volume (V), where R is the gas constant. From the slope and interception of such isotherms, ΔH and V can be computed. After calculation of the activation parameters, a referenced temperature was chosen ($T_{ref} = 40°C$), and the horizontal and vertical shifts were determined to build a master curve at the referenced temperature. The others parameters m, n, $\dot{\varepsilon}_0$, $\sigma_i(0)$ are obtained when the best fit of the master curve is obtained [19]. Knowing the activated parameter of DAPA, and

the master curve of DAPAC (built at the same reference temperature) at different cellulose concentrations, the effective activated parameters for DAPAC composite can be calculated according to eq (3). From the ΔH_{eff} value, the parameters ΔH_D and ΔH_C could be estimated through Equation (3) for a given cellulose content. The remaining cooperative model parameters (V_{eff} , n, $\dot{\varepsilon}_0$) are then calculated with a fit of the master curve. Finally, the parameters V_D and V_C are also derived from Equation (3).

A previous publication [16] can be used as a reference to estimate the yield stress of DAPA and DAPAC, obtained in tension and at low strain rate. The master curves created at 40°C with DAPA and DAPAC5 are given in Fig 9. The parameters obtained for the best fit of master curve are shown in Table 2. Table 3 presents the evolution of the activations parameters with the cellulose content. The reported values mentioned a slight increase of the activation energy with the cellulose content, and a slight decrease of the activation volume with increasing cellulose concentration. These results are in agreement with the experimental results where the yield stress increases with the filler content concentration. Fig 10 shows the reduced yield stress (σ_y / T , versus log ($\dot{\varepsilon}$)) plots for DAPA and DAPAC composites. The cooperative model predictions of the yield stress are in good agreement with the experimental data, showing that the plastic flow is controlled by the cooperative motion of the chain segments, and obey to strain rate and temperature superposition principle.

4. CONCLUSION

Dynamic compressive behaviour of DAPA and the corresponding biocomposites based on pure cellulose fibres have been studied using split Hopkinson pressure bars (SHPB). The incorporation of cellulose fibres leads to an increase of the Young's modulus, the yield stress and

the flows stress. Both Young's modulus and yield stress increase with the CF content. Both, DAPA and DAPAC are very sensitive to the strain rate and to the temperature. These systems present a very marked strain hardening at high strain rate. As the strain rate increases, the effect of strain hardening decreases slightly for high fibre content. These systems maintain their ability to plastically deform. A study of the compressive yield behaviour with cooperative model showed that the activation energy increases slightly with the CF concentration, whereas the activation volume decreases slightly with increasing CF concentration. The model predictions of the yield stress are in good agreement with the experimental data.

The association of a bio-based polymer with cellulose fillers is a good answer to overcome primary issues with green polymers, i.e. the material cost and the mechanical properties. This study brings significant information for the applications considered for these materials, e.g. automobile or coating industry. In addition, these materials are in good agreement with the emergent concept of sustainable development.

ACKNOWLEDGMENTS

The authors thank Prolea for providing dimer acid. Thanks are also extended to the ANRT and the Région Alsace for financial support.

REFERENCES

[1] Patel M, Bartle I, Bastioli C, Doutlik K, Ehrenberg J, Johansson D, Kab H, Klumpers J, Luther R, Wittmeyer D. Towards the integration of renewable raw materials in EU climate policy. Part 1. Agro Food Ind. Hi-Tech 2002;13:28.
[2] Carlsson AS. Plant oils as feedstock alternatives to petroleum - A short survey of potential oil crop platforms. Biochimie 2009;91:665.
[3] Lu Y, Larock RC. Novel polymeric materials from vegetable oils and vinyl monomers: Preparation, properties, and applications. ChemSusChem 2009;2:136.
[4] Meier MAR, Metzger JO, Schubert US. Plant oil renewable resources as green alternatives in polymer science. Chem. Soc. Rev. 2007;36:1788.
[5] Petrovic ZS. Polyurethanes from vegetable oils. Polymer Reviews 2008;48:109.
[6] Sharma V, Kundu PP. Condensation polymers from natural oils. Prog. Polym. Sci. 2008;33:1199.
[7] Williams CK, Hillmyer MA. Polymers from Renewable Resources: A Perspective for a Special Issue of Polymer Reviews. Polym. Rev. 2008;48:1.
[8] Hablot E, Zheng D, Bouquey M, Averous L. Polyurethanes Based on Castor Oil: Kinetics, Chemical, Mechanical and Thermal Properties. Macromol. Mater. Eng. 2008;293:922.
[9] Cavus S, Gurkaynak MA. Influence of monofunctional reactants on the physical properties of dimer acid-based polyamides. Polym. Adv. Technol. 2006;17:30.
[10] Chen XM, Zhong H, Jia LQ, Ning JC, Tang RG, Qiao JL, Zhang ZY. Polyamides derived from piperazine and used for hot-melt adhesives: synthesis and properties. Int. J. Adhes. 2002;22:75.
[11] Hablot E, Donnio B, Bouquey M, Averous A. "Dimer acid-based thermoplastic bio-polyamides: Reaction kinetics, properties and structure." Polymer 2010;51:5895.
[12] Chen X, Zhong H, Jia L, Ning J, Tang R, Qiao J, Zhang Z. Polyamides derived from piperazine and used for hot-melt adhesives: synthesis and properties. Int. J. Adhes. 2002;22:75.
[13] Fan XD, Deng YL, Waterhouse J, Pfromm P. Synthesis and characterization of polyamide resins from soy-based dimer acids and different amides. J. Appl. Polym. Sci. 1998;68:305.
[14] Fan XD, Deng YL, Waterhouse J, Pfromm P, Carr WW. Development of an easily deinkable copy toner using soy-based copolyamides. J. Appl. Polym. Sci. 1999;74:1563.
[15] Hablot E, Matadi R, Ahzi S, Avérous L. Renewable biocomposites of dimer fatty acid-based polyamides with cellulose fibres: Thermal, physical and mechanical properties. Compos. Sci. Technol. 2010;70:504.
[16] Hablot E, Matadi R, Ahzi S, Vaudemond R, Ruch D, Avérous L. Yield behaviour of renewable biocomposites of dimer fatty acid-based polyamides with cellulose fibres. Compos. Sci. Technol. 2010;70:525.
[17] Miyagawa H, Misra M, Drzal LT, Mohanty AK. Fracture toughness and impact strength of anhydride-cured biobased epoxy. Polym. Eng. Sci. 2005;45:487.
[18] Miyagawa H, Mohanty AK, Misra M, Drzal LT. Thermo-physical and impact properties of epoxy containing epoxidized linseed oil, 2: Amine-cured epoxy. Macromol. Mater. Eng. 2004;289:636.
[19] Miyagawa H, Mohanty AK, Misra M, Drzal LT. Thermo-physical and impact properties of epoxy containing epoxidized linseed oil, 1: Anhydride-cured epoxy. Macromol. Mater. Eng. 2004;289:629.

[20] Liu ZS, Erhan SZ, Calvert PD. Solid freeform fabrication of epoxidized soybean oil/epoxy composites with di-, tri-, and polyethylene amine curing agents. J. Appl. Polym. Sci. 2004;93:356.
[21] Song B, Chen W, Liu Z, Erhan S. Compressive properties of epoxidized soybean oil/clay nanocomposites. Int. J. Plast. 2006;22:1549.
[22] Song B, Chen W, Liu Z, Erhan SZ. Compressive properties of soybean oil-based polymers at quasi-static and dynamic strain rates. J. Appl. Polym. Sci. 2006;99:2759.
[23] Reid SR, Peng C. Dynamic uniaxial crushing of wood. Int. J. Impact Eng. 1997;19:531.
[24] Holmgren SE, Svensson BA, Gradin PA, Lundberg B. An encapsulated split hopkinson pressure bar for testing of wood on elevated strasin rate, temperature, and pressure. Exp. Tech. 2008;32:44.
[25] Chivrac F, Gueguen O, Pollet E, Averous L, Ahzi S, Belouettar S. Micromechanically-based formulation of the cooperative model for the yield behavior of starch-based nano-biocomposites. J. Nanosci. Nanotechnol. 2010;10:2949.
[26] Gueguen O, Richeton J, Ahzi S, Makradi A. Micromechanically based formulation of the cooperative model for the yield behavior of semi-crystalline polymers. Acta Mater. 2008;56:1650.
[27] Matadi R, Gueguen O, Ahzi S, Gracio J, Muller R, Ruch D. Investigation of the stiffness and yield behaviour of melt-intercalated poly(methyl methacrylate)/organoclay nanocomposites: Characterisation and modelling. J. Nanosci. Nanotechnol. 2010;10:2956.
[28] Richeton J, Ahzi S, Daridon L, Rémond Y. A formulation of the cooperative model for the yield stress of amorphous polymers for a wide range of strain rates and temperatures. Polymer 2005;46:6035.
[29] Amash A, Zugenmaier P. Morphology and properties of isotropic and oriented samples of cellulose fibre-polypropylene composites. Polymer 2000;41:1589.
[30] Matadi R, Makradi A, Ahzi S, Sieffert JG, Etienne S, Rush D, Vaudemont R, Muller R, Bouquey M. Preparation, structural characterization and thermomechanical properties of poly(methyl methacrylate)/ organoclay nanocomposites by melt intercalation. J. Nanosci. Nanotechnol. 2009;9:2923.
[31] Pessey D, Bahlouli N, Pattofatto S, Ahzi S. Polymer composites for the automotive industry: Characterisation of the recycling effect on the strain rate sensitivity. Int. J. Crashworthiness 2008;13:411.
[32] Grote DL, Park SW, Zhou M. Dynamic behavior of concrete at high strain rates and pressures: I. experimental characterization. Int. J. Impact Eng. 2001;25:869.
[33] Buckley CP, Harding J, Hou JP, Ruiz C, Trojanowski A. Deformation of thermosetting resins at impact rates of strain. Part I: Experimental study. J. Mech. Phys. Solids 2001;49:1517.
[34] Walley SM, Field JE, Pope PH, Safford NA. Philosophical Transactions of the Royal Society of London. Series A, Mathematical and Physical Sciences 1989;328:1.
[35] Chen LP, Yee AF, Moskala EJ. The Molecular Basis for the Relationship between the Secondary Relaxation and Mechanical Properties of a Series of Polyester Copolymer Glasses. Macromol. 1999;32:5944.
[36] Guo Y, Li Y. Quasi-static/dynamic response of SiO2-epoxy nanocomposites. Mater. Sci. Eng., A 2007;45:330.
[37] Takyanagi M, Uemura S, Minami S. Application of equivalent model method to dynamic rheo-optical properties of crystalline polymer. J. Polym. Sci.: Part C: Polym. Lett. 1964;5:113.

FIGURES CAPTION

Fig. 1. Scanning electron micrographs of the cryogenic fracture surfaces of DAPAC15

Fig. 2. Experimental true stress versus true strain curves under uniaxial compression loading at 20 °C, with 4 true strain rates. (strain Rate 1=413 ± 6.2%, , Strain Rate 2=913 ± 4.2%, Strain Rate 3=1735 ± 2.3% , Strain Rate 4=2730 ± 2.7%)

Fig 3. Experimental true stress versus true strain curves under uniaxial compression loading at 40 °C, with 4 true strain rates (strain Rate 1=413 ± 6.2%, , Strain Rate 2=913 ± 4.2%, Strain Rate 3=1735 ± 2.3% , Strain Rate 4=2730 ± 2.7%)

Fig 4. Experimental true stress versus true strain curves under uniaxial compression loading at 60 °C, with 4 true strain rates (strain Rate 1=413 ± 6.2%, , Strain Rate 2=913 ± 4.2%, Strain Rate 3=1735 ± 2.3% , Strain Rate 4=2730 ± 2.7%)

Fig 5. Optical micrograph of DAPAC10 (magnification X2)

Fig 6. Experimental true stress versus true strain curves under uniaxial compression loading at 20 and 60 °C, with 4 true strain rates (strain Rate 1=413 ± 6.2%, , Strain Rate 2=913 ± 4.2%, Strain Rate 3=1735 ± 2.3% , Strain Rate 4=2730 ± 2.7%)

Fig 7. The dependence of Young's modulus in dynamic compression on strain rate at 3 temperatures

Fig 8. The dependence of yield stress in dynamic compression on strain rate, at 3 different temperatures (20, 40 and 60 °C)

Fig 9. Master curve of DAPA and DAPAC5 build at a reference temperature of 313K

Fig 10. yield stress/Temperature versus strain rate of DAPA and DAPAC5

Tables

Table 1
Strain-rate, fibre-weight and temperature effects on yield stress and Young's modulus (strain Rate 1=413 ± 6.2%, , Strain Rate 2=913 ± 4.2%, Strain Rate 3=1735 ± 2.3% , Strain Rate 4=2730 ± 2.7%)

Weight	Temperature	Young's modulus (MPa)				Yield stress (MPa)			
		Strain rate (s^{-1})				Strain rate (s^{-1})			
		1	2	3	4	1	2	3	4
0%	20°C	465	514	555	603	31	45	51	60
	40°C	249	303	353	549	20	36	48	56
	60°C	83	106	126	143	6	15	18	22
5%	20°C	541	559	651	748	35	53	62	66
	40°C	306	344	468	622	23	39	51	60
	60°C	106	169	205	320	8	17	20	25
10%	20°C	611	644	753	891	39	58	73	76
	40°C	332	422	532	764	25	45	55	73
	60°C	146	213	325	464	12	22	33	36
15%	20°C	695	790	942	1006	43	67	79	83
	40°C	430	541	655	840	29	48	62	76
	60°C	194	245	296	560	14	26	36	45

Table 2
Cooperative model parameters

Parameters	Value
DAPA	
n	6
φ	0.81
$\dot{\varepsilon}_0$	7.6E+22
$\sigma_i(0)$ (MPa)	1.9
m	0.0067
$\rho_{m\,(}\, g/cm^3)$	0.90
T_{ref} (K)	313
$V_D\ (m^3)$	1.17E-27
$\Delta H_D\ (kJ/mol)$	127.4
DAPAC	
$\rho_{c\,(}\, g/cm^3)$	1.5
$V_C\ (m^3)$	9.52E-28
$\Delta H_C\ (kJ/mol)$	351.46

Table 3
Variation of effective parameters with the cellulose concentration

Cellulose concentration (wt %)	*Volume fraction*	ΔH_{eff} *(kJ/mol)*	V_{eff} (m^3)
0	0	127.4	1.17E-27
5	3.17E-3	130.7	1.10E-27
10	6.34E-3	134.1	1.08E-27
15	9.55E-3	134.3	1.07E-27